

SEISMIC WHEEL for SHALLOW CHARACTERIZATION (0- 1 m) OF SOILS ON THE MOON AND MARS: J. M. Lorenzo¹, C. Sun², D. A. Patterson¹, W. Stryjewski¹, S. Karunatillake¹, H. Haviland³, M. Zanetti³, R. C. Weber³, C. Fassett³, ¹Dept. Geology and Geophysics, Louisiana State University, Cnr. Tower and S. Campus Drives, Baton Rouge, LA 70803, gllore@lsu.edu., ²Dept. Civil and Environmental Engineering, LSU ³NASA Marshall Space Flight Center, 320 Sparkman Drive, Huntsville, AL 35805, heidi.haviland@nasa.gov.

Introduction: Water-ice on Mars and Moon is an essential resource to fuel and water future human explorers. The distribution of shallowly buried ice can also help constrain the relative roles of precipitation, brines, and obliquity cycles on Mars [1]. The relative roles of geologic processes – such as impact gardening – in determining the distribution of ground ice in lunar

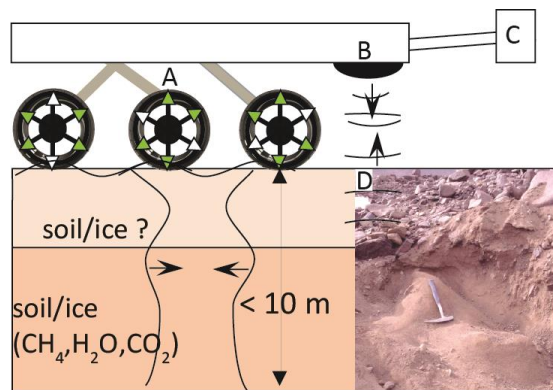


Figure 1. A. Alternating piezo-ceramic sensors (green) and sources (white) receive and transmit surface waves through wheel structure (not to scale) B. GPR transceiver detects pore-space substituted with ice and C. A long-arm GRNS sensor collects background compositional energies away from influence of rover. D. As a specific example for Mars, Antarctic Dry Valley analog [2] implies a potentially complex soil-ice mixture for Mars that requires an integrated suite of geophysical and geochemical tools.

permanently shadowed regions likewise remains poorly explored [3]. Recent, martian, mid-latitude ice discoveries emphasize these areas as key to future exploration [2]. Non-invasive in-situ characterization can be the key to modeling the geology of ground ice and advancing prior remote and in situ observations. An optimal rover-based integrated approach for the purpose combines (1) high-frequency seismic (kHz) (2) ground-penetrating radar as well as (3) nuclear spectroscopy in order to provide exploratory information about the spatial distribution, depth, density, nature of overburden, and distinct layering of ice deposits within an area of interest (Fig. 1).

Because of its small weight (10^3 g), size (cm^3) and durability, a combined piezoceramic-based, high-frequency (kHz) pulser-source and accelerometer

combination seismometer subsystem may provide an acoustic sub-system capable of adaptive mounting to the wheels of autonomous exploratory rovers (Fig. 1).

Seismic Wheel Tests We conduct preliminary evaluations of the vibrational performance of wheel-mounted accelerometers. Along the rim interior of a

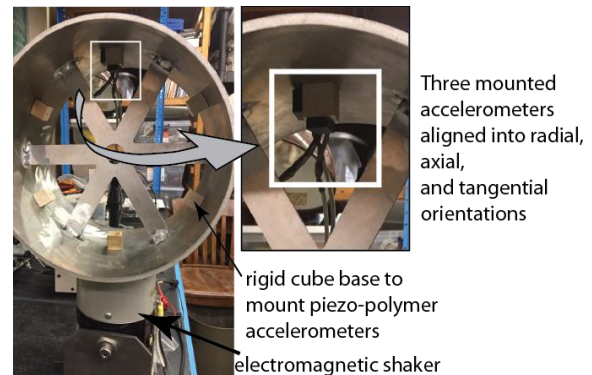


Figure 2. Six sensor stations, every 60° mounted to the interior of a mock rover wheel. Each station holds 3 accelerometers. Shaker motion is vertical and ranges between 10 Hz – 10 kHz.

mock rover wheel, we place six (6) equally spaced every 60°. At each station we place 3 single-component accelerometers. An electromagnetic shaker oscillates the rigidly attached wheel over a

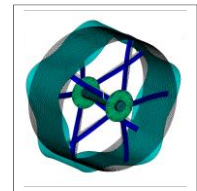


Figure 3 We use a meshed wheel finite element model: diameter = 250 mm ; width = 100 mm. Thickness of the grouser = 2.5mm; diameter of the central shaft= 5 mm. Parts of the wheel are modeled using aluminum (Young's modulus=69 GPa, density = 2700 kg/m³, Poisson's ratio = 0.33). The spoke has a cross-section =10x10 mm². Simply supported boundary conditions are applied at the two ends of the central shaft with no external loading.

broad frequency range of 10 to 10 kHz. Amplitudes vary sinusoidally and all motion is vertical (Fig. 2). Numerical, finite element modeling of an equivalent, meshed wheel predicts multiple resonant frequencies and modes of deformation (Fig. 3) and is used as a theoretical reference.

Spectral Response of Sensors on Wheel: Spectral responses of the 8 accelerometers are similar and show common, key characteristics. (1) Amplitudes of radial and tangential components dominate axial components (Fig. 4). Dominant resonance peaks occur at 20 Hz (from the shaker during testing) and starting above 700 Hz (+ 10dB). These initial results suggest that all portions of the mock-wheel can act in unison as a seismic receiver at nominally expected wavelengths. For example, sound at 100 Hz in a granular medium (soil, regolith) which displays seismic velocities of 100 m/s [4], [5] has a wavelength ~ 100 cm. If during field

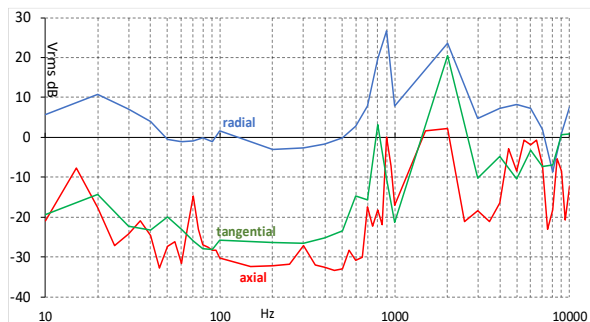


Figure 4. A representative, 3-component spectral response of wheel-mounted piezo-accelerometers. Vertical axis is V_{rms} and horizontal, logarithmic axis displays shaking frequency. As expected, the strongest response occurs in the vertical direction (radial) Natural resonances in the shaker-wheel-sensor system center > 900 Hz. In this preliminary test, useful seismic bandwidth (0 to -20 dB) exists < 1000 Hz. Similar behavior is noted at 6 other locations about wheel. Resonance at 20 Hz is shaker-induced.

deployment, only a relatively small portion (est. 20%, of ~ 80 cm) of the rigid outer wheel contacts the ground, the effective portion of the surface wavelength sampled by contact is $< 1/5$ dominant wavelength. Seismic resolution is potentially better as velocities increase and because the accelerometer bandwidth extends into the kHz region. Seismic properties also directly relate to ice-cementation rigidity, lateral continuity, and attenuation (inversely related to ice quantity).

Recent seismic results [6],[7] dealing with laboratory-based analyses, indicate that seismic attenuation in soil analogs improves with ice concentration and that seismic surface waves can robustly provide values for the elastic moduli of the underlying units. We note that the signal shape and size of the piezo-pulser can be readily changed electrically.

Signal Shaping: Solutions to acoustic resonance can be considered during early stages of wheel design. As well, the spectral (frequency, phase) responses of the

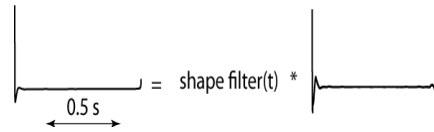


Figure 5. A shape filter is a standard method to reduce potential predictable resonances embedded in seismic data. The resonance-free, desired signal (left) is reconstructed from the vibrational test data. The signal with resonance (right) is synthesized from phase and amplitude vibrational data (e.g., Fig. 4).

wheel can be deconvolved from the seismic data to extract accurate signals. That is, optimum Wiener filters [8] can help distinguish systematic, noise from seismic signals (Fig. 5).

Summary and Conclusions: The Spectral response of accelerometers mounted on a mock rover wheel (Figs. 2, 4) appears to display a minimum usable bandwidth of ~ 700 Hz (Fig. 4). Similar usable bandwidths at all stations along the wheel perimeter. Future wheel designs may benefit by favoring seismic behavior.

We use seismic piezo-sensors and piezo-sources that are one order of magnitude broader in bandwidth (kHz) and resolution than the current Mars InSight [5] short-period seismometer (~ 50 Hz), and better suited for investigating the shallow soils (< 10 m). Piezo-ceramics endured and performed successfully in space on the Cassini-Huygens probe to Titan e.g.,[8]. Cryogenic, commercial off-the shelf piezo-units are readily available with low power consumption (μA) and low mass (9 g).

If we assume 100 m/s for shallow Mars soils and shallow lunar regolith the raw seismic response of the wheel should be relatively resonance-free for wavelengths of order ~ 1 m or less. Rigid metal wheel components close to the outer perimeter are recommended for sensor placement.

Acknowledgments: Support from NASA EPSCoR Cooperative agreement 80NSSC20M0150 (CFDA #43.008).

References: [1] Karunatillake et al., http://surveygizmoreponseuploads.s3.amazonaws.com/fileuploads/623127/5489366/252-12a3f13b4954afb9332f2d6978dae999_KarunatillakeSuniti.pdf [2] Heldmann, et al., (2013) *Planet. Space Sci.*, 85, 53–58. [3] Cannon, K. M., & Britt, D. T. (2020). *Icarus*, 347(March). [4] Cooper, et al., (1974) *Reviews of Geophysics*, 12, 3, 291-308. [5] Lognonné, P., et al. (2020). *Nature Geoscience* 13(3) 213-220. [6] Lorenzo, J. M., et al. (2020). NASA/TM–2020500352041-49. [7] Lorenzo, J. M., et al, (2019) *LPS L*, Abstract #3246. [8] Robinson and Treitel, (1980) *Geophysical signal analysis*: Prentice-Hall Book Co [9] Zarnecki, J., et al. (2005) *Nature* 438,792–795.